A Two-Dimensional One Component Plasma and a Test Charge: Polarization Effects and Effective Potential

Gabriel Téllez · Emmanuel Trizac

Abstract We study the effective interactions between a test charge Q and a one-component plasma, i.e. a complex made up of mobile point particles with charge q, and a uniform oppositely charged background. The background has the form of a flat disk, in which the mobile charges can move. The test particle is approached perpendicularly to the disk, along its axis of symmetry. All particles interact by a logarithmic potential. The long and short distance features of the effective potential—the free energy of the system for a given distance between Q and the disk—are worked out analytically in detail. They crucially depend on the sign of Q/q, and on the global charge borne by the discotic complex, that can vanish. While most results are obtained at the intermediate coupling $\Gamma \equiv \beta q^2 = 2$ (β being the inverse temperature), we have also investigated situations with stronger couplings: $\Gamma = 4$ and 6. We have found that at large distances, the sign of the effective force reflects subtle details of the charge distribution on the disk, whereas at short distances, polarization effects invariably lead to effective attractions.

**Keywords** Coulomb systems · Colloids · Overcharging · Polarization

1 Introduction

Electric charges are ubiquitous in the colloidal domain, and often a major player shaping the behaviour of soft matter systems. Counter-intuitive phenomena often ensue, such as over-charging (charge inversion) or effective attraction between like-charged macro-ions [1–7]. To rationalize such observations that are the fingerprints of correlation effects, simplified models are welcome, that should furthermore be treated beyond the mean-field level [8]. Interestingly, the physics of strongly coupled charged systems has witnessed relevant progress

G. Téllez (✉)
Departamento de Física, Universidad de Los Andes, A.A. 4976, Bogotá, Colombia
e-mail: gtellez@uniandes.edu.co

E. Trizac
Laboratoire de Physique Théorique et Modèles Statistiques, UMR CNRS 8626, Université Paris-Sud, 91405 Orsay, France
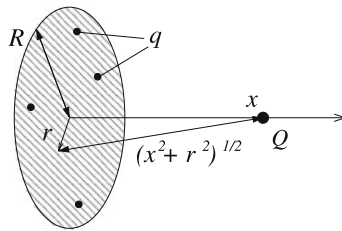
Fig. 1 Definition of the system under consideration: a disk $\mathcal{D}$ with fixed and uniform background charge (*hatched area*), in which N mobile oppositely charged particles, shown by the *bullets*, are free to move ($N = 4$ in the figure). The total charge of the background is $-N_b q$, while each mobile ion bears a charge q. The total charge on the disk (background plus free ions) is therefore $(N - N_b)q$. A test ion with charge Q approaches the disk along the symmetry axis shown, defining x-coordinate ($x = 0$ when the test charge lies on the disk, at the center)

in the last 15 years [4, 9–13], while the study in the weak coupling limit where mean-field arguments hold, started about 100 years ago [14, 15]. The study of intermediate Coulombic couplings, though, appears more elusive [16–19] and will be the focus of our interest in the present paper.

The system under scrutiny here is a variant of Thomson's plum pudding model (see [20–22] and references therein), also referred to as the One Component Plasma [4, 23, 24]. Point particles with charge q are embedded in a two-dimensional flat disk $\mathcal{D}$ of radius R. In addition, a uniformly charged background is present in the disk region (see Fig. 1). While the charged background is fixed, the particles are free to move in $\mathcal{D}$. They interact through a log potential, the form taken by Coulomb law in two dimensions. The relevant coupling parameter is $\Gamma = \beta q^2$, where β is the inverse temperature. At small Γ (formally $\Gamma \to 0$), the Poisson-Boltzmann mean-field description holds [25].[1]

As is often the case for 2D Coulombic problems, the coupling parameter $\Gamma = 2$ lends itself to an exact analytical treatment, see Refs. [24, 26, 27]. The goal is here to extend the exact analysis at $\Gamma = 2$ to investigate the interactions between the disk bearing the mobile charges, and a test charge Q that is approached perpendicularly to the disk, along the axis of symmetry (see Fig. 1). We shall assume that Q and all other charges (mobile + background) interact through a log potential. Since Q explores a third additional direction compared to those in which the point q-charges and the background disk are confined, the choice of such a potential can be questioned: it does not correspond to the solution of Poisson's equation in three dimensions. This is however the price for obtaining analytical results, that shed light on phenomena at work in more realistic systems. In particular, we will be interested in the effective interactions between the fixed charge Q and other charges, that can be seen as mimicking a colloid (the uniform background), dressed by a double-layer of counterions (the mobile q-charges).

The model will be defined in Sect. 2, where the theoretical tools will also be introduced. In Sect. 3, the features of the effective potential at large distances will be addressed. While most of the present analysis pertains to the $\Gamma = 2$ case, other couplings will be addressed

---

[1]It is straightforward to check that in the globally neutral case $N = N_b$, the mean-field solution is trivial, with a vanishing electrostatic potential, and a particle density that compensates for that of the background. This is a consequence of the confinement in $\mathcal{D}$ imposed to the charges. If the mobile charges are allowed to leave the uniformly charged disk and explore the whole 2D plane, the mean-field solution becomes non trivial—the constant electrostatic potential can by no means provide a solution to the problem—and has been studied in [42, 49]. We come back to this modified "unbounded" model in our concluding section.

(namely $\Gamma = 4$ and 6, corresponding to smaller temperatures). Then, the emphasis will be in Sect. 4 on short range correlations that, through polarization effects, rule the short distance behaviour of the effective potential. Conclusions will be drawn in Sect. 5.

2 Model and General Formalism

The system is a one-component plasma [23, 24, 26, 28] on a disk $\mathcal{D}$ of radius R with N mobile point charges q, and a fixed background charge density $\rho_b = -qn_b$. The system can be globally charged, since $N_b = \pi R^2 n_b$ can be different from N. The charged particles interact with the two-dimensional logarithmic Coulomb potential,

$$v_c(\mathbf{r}_i, \mathbf{r}_j) = -\ln \frac{|\mathbf{r}_i - \mathbf{r}_j|}{\ell},\tag{1}$$

for two particles located at $\mathbf{r}_i$ and $\mathbf{r}_j$ on the disk (ℓ is an arbitrary length). The interaction potential between a charge q located at $\mathbf{r}$ and the background consequently reads

$$v_b(r) = \int_{\mathcal{D}} q\rho_b v_c(\mathbf{r}, \mathbf{r}')\, d^2\mathbf{r}' = \frac{\pi n_b q^2}{2}\left[r^2 - R^2\left(1 - 2\ln\frac{R}{\ell}\right)\right],\tag{2}$$

where $r = |\mathbf{r}|$. The disk is in thermal equilibrium with a heat bath at an inverse temperature $\beta = 1/k_B T$. We consider now that a particle with charge Q approaches the disk from the axis normal to the disk that passes through its center, see Fig. 1. The charge Q is held fixed at a distance x from the disk. The interaction potential between this charged particle and a charge from the disk located at $\mathbf{r}$, will also be taken logarithmic:

$$v_Q(x, r) = -\ln \frac{\sqrt{x^2 + r^2}}{\ell}.\tag{3}$$

It will be convenient to use rescaled lengths $\widetilde{r} = \sqrt{\pi n_b}\, r$, $\widetilde{x} = \sqrt{\pi n_b}\, x$, $\widetilde{\ell} = \sqrt{\pi n_b}\,\ell$, etc. With such a choice, the rescaled disk radius is $\widetilde{R} = \sqrt{N_b}$. The interaction potential between the background and the approaching particle is

$$
\begin{aligned}
V_{Qb}(x) &= \int_{\mathcal{D}} Q\rho_b v_Q(x, r)\, d^2\mathbf{r} \\
&= \frac{Qq}{2}\left[(N_b + \widetilde{x}^2)\ln(N_b + \widetilde{x}^2) - N_b - \widetilde{x}^2 \ln \widetilde{x}^2\right],
\end{aligned}\tag{4}
$$

where we have chosen the arbitrary constant ℓ such that $\widetilde{\ell} = 1$.

2.1 The Special Coupling $\Gamma = 2$

Since the one-component plasma on the disk is two-dimensional with log-potential, one can use the special techniques developed for two-dimensional Coulomb systems [24, 26] and random matrices [29] to compute exactly the effective interaction potential between the disk and the approaching charge, for a special value of the Coulomb coupling $\Gamma = \beta q^2 = 2$.

Let $\mathbf{r}_i$ be the position of the i-th particle on the disk, in polar coordinates $\mathbf{r}_i = (r_i, \varphi_i)$. It is convenient to define $z_i = r_i e^{i\varphi_i}$ and $\widetilde{z}_i = \widetilde{r}_i e^{i\varphi_i}$. The total potential energy of the system can be written, up to an irrelevant constant

$$H = Qq \sum_{i=1}^{N} v_Q(x, r_i) + V_{Qb}(x) + \frac{q^2}{2} \sum_{i=1}^{N} \widetilde{r}_i^2 - q^2 \sum_{1 \le i < j \le N} \ln |\widetilde{z}_i - \widetilde{z}_j|,\tag{5}$$

where the first two terms on the right hand side account for the test charge—mobile charge and test charge—background interactions respectively, while the last two terms are for the mobile charge—background and mobile charge—mobile charge energies. When $\beta q^2 = 2$, up to a multiplicative constant, the Boltzmann factor reads

$$e^{-\beta H} = e^{-\beta V_{Qb}(x)} \prod_{i=1}^{N} e^{-2\frac{Q}{q} v_Q(x,r_i) - \tilde{r}_i^2} \prod_{1 \le i < j \le N} |\tilde{z}_i - \tilde{z}_j|^2. \tag{6}$$

The product $\prod_{1 \le i < j \le N} (\tilde{z}_i - \tilde{z}_j)$ is a Vandermonde determinant $\det(\tilde{z}_i^{j-1})$. Defining

$$\psi_j(\mathbf{r}) = e^{-\frac{Q}{q} v_Q(x,r) - \frac{\tilde{r}^2}{2}} \tilde{z}^j, \tag{7}$$

the Boltzmann factor can be written as

$$e^{-\beta H} = e^{-\beta V_{Qb}(x)} \left| \det(\psi_{j-1}(\mathbf{r}_i))_{1 \le i,j \le N} \right|^2. \tag{8}$$

The functions ψ_j are orthogonal

$$\int_{\mathcal{D}} \overline{\psi_j(\mathbf{r})} \psi_k(\mathbf{r}) \, d^2\mathbf{r} = 0 \quad \text{if } j \ne k, \tag{9}$$

with norm

$$\|\psi_j\|^2 = \int_{\mathcal{D}} |\psi_j(\mathbf{r})|^2 \, d^2\mathbf{r} = \frac{1}{n_b} \int_0^{N_b} t^j (\tilde{x}^2 + t)^{Q/q} e^{-t} \, dt. \tag{10}$$

If Q/q is a positive integer, this can be expressed in terms of incomplete gamma functions $\gamma(k, N_b) = \int_0^{N_b} t^{k-1} e^{-t} \, dt$. For instance, when $Q = q$,

$$\|\psi_j\|^2 = \frac{1}{n_b} \left[\tilde{x}^2 \gamma(j+1, N_b) + \gamma(j+2, N_b) \right]. \tag{11}$$

The configurational canonical partition function is

$$Z = \frac{1}{N!} \int_{\mathcal{D}^N} e^{-\beta H} \prod_{i=1}^{N} d^2\mathbf{r}_i$$

$$= \frac{1}{N!} e^{-\beta V_{Qb}(x)} \int_{\mathcal{D}^N} \left| \det(\psi_{j-1}(r_i))_{1 \le i,j \le N} \right|^2 \prod_{i=1}^{N} d^2\mathbf{r}_i. \tag{12}$$

If the determinant is explicitly expanded, and the integrals performed, the result simplifies [26, 29], due to the orthogonality of the functions ψ_j

$$Z = e^{-\beta V_{Qb}(x)} \prod_{j=0}^{N-1} \|\psi_j\|^2. \tag{13}$$

Up to an additive constant, the effective interaction potential, $V_{\text{eff}}(x)$, between the disk and the approaching charge Q, is given by [30] $e^{-\beta V_{\text{eff}}(x)} \propto Z$, and more specifically, we choose

$$e^{-\beta V_{\text{eff}}(x)} = \frac{Z}{Z_0}, \tag{14}$$

where Z_0 is the x-independent partition function when $Q = 0$. The above definition ensures that for $N = N_b$, $V_{\text{eff}}(x) \to 0$ when $x \to \infty$. On the other hand, for $N \ne N_b$, $V_{\text{eff}}(x)$ diverges for $x \to \infty$, see below. The physical meaning of V_{eff} is clear: $-\partial V_{\text{eff}}(x)/\partial x$ provides

the mean force experienced by Q, averaged over all possible fluctuations of charge configurations on the disk. The function V_{eff} is precisely the free energy of the system, for a given test charge—disk distance x. Therefore,

$$\beta V_{eff}(x) = \frac{Q}{q}\left[(N_b + \widetilde{x}^2)\ln(N_b + \widetilde{x}^2) - N_b - \widetilde{x}^2\ln\widetilde{x}^2\right]$$
$$- \sum_{j=1}^{N}\left[\ln\int_0^{N_b} t^{j-1}(\widetilde{x}^2 + t)^{Q/q}e^{-t}\,dt - \ln\gamma(j, N_b)\right]. \tag{15}$$

In the special case $Q = q$, we obtain

$$\beta V_{eff}(x) = (N_b + \widetilde{x}^2)\ln(N_b + \widetilde{x}^2) - N_b - \widetilde{x}^2\ln\widetilde{x}^2$$
$$- \sum_{j=1}^{N}\ln\left[\widetilde{x}^2 + \frac{\gamma(j+1, N_b)}{\gamma(j, N_b)}\right]. \tag{16}$$

The density profile $n(r)$ on the disk can also be obtained explicitly [24, 29], and will be discussed in some detail below

$$n(r) = \sum_{j=0}^{N-1}\frac{|\psi_j(\mathbf{r})|^2}{\|\psi_j\|^2} = n_b\sum_{j=0}^{N-1}\frac{\widetilde{r}^{2j}(\widetilde{x}^2 + \widetilde{r}^2)^{Q/q}\,e^{-\widetilde{r}^2}}{\int_0^{N_b} t^j(\widetilde{x}^2 + t)^{Q/q}\,e^{-t}\,dt}. \tag{17}$$

It can be checked that the two situations where $Q = 0$ and $x \to \infty$ are equivalent, since both decouple the test charge from those on the disk.

2.2 Arbitrary Even Coupling Parameters

For couplings parameters $\Gamma = \beta q^2 = 2\gamma$, with γ an integer, the partition function of the system, and the effective potential, can be computed for small enough number of particles N, by using a method developed in [31, 32], based on techniques used in the study of the quantum Hall effect [33–35]. We provide here some details on the methods.

Up to a multiplicative constant, the Boltzmann factor of the system reads

$$e^{-\beta H} = e^{-\beta V_{Qb}(x)}\left|\det(\psi_{j-1}(r_i))_{1\leq i,j\leq N}\right|^{2\gamma}. \tag{18}$$

where, now, the orthogonal functions ψ_k are

$$\psi_k(\mathbf{r}) = [w(r)]^{1/2}\bar{z}^k \tag{19}$$

with

$$w(r) = e^{-2\gamma\frac{Q}{q}v_Q(x,r)-\gamma\widetilde{r}^2}. \tag{20}$$

The key idea to compute the partition function is to expand $[\det(\bar{z}_k^{j-1})]^{\gamma}$ in terms of appropriate orthogonal polynomials [32]. For γ even, the expansion is in terms of symmetric monomials, whereas for γ odd, it is expanded in terms of antisymmetric polynomials. The coefficients of the expansion are conveniently indexed by a partition $\mu = (\mu_1, \ldots, \mu_N)$ of $\gamma N(N-1)/2$, for example for γ even,

$$\left[\det(\bar{z}_k^{j-1})\right]^{\gamma} = \sum_{\mu} c_{\mu}\,\mathrm{Sym}(z_1^{\mu_1}\ldots z_N^{\mu_N}) \tag{21}$$

with the symmetric monomial

$$\mathrm{Sym}(z_1^{\mu_1}\ldots z_N^{\mu_N}) = \frac{1}{\prod_i m_i!}\sum_{\sigma\in S_N} z_{\sigma(1)}^{\mu_1}\ldots z_{\sigma(N)}^{\mu_N} \tag{22}$$

where S_N is the permutation group of N elements and m_i is the multiplicity of the integer i in the partition μ. A similar expression is used for γ odd with antisymmetrized monomials.

Due to the orthogonality of the (anti)symmetric monomials, the partition function is finally given also as an expansion similar to the one of the power γ of the Vandermonde determinant, see [32] for details. The final expression for the effective potential is

$$\beta V_{\text{eff}}(x) = \beta V_{Qb}(x) - \ln \frac{Z^*}{Z_0^*} \tag{23}$$

with

$$Z^* = \sum_\mu \frac{c_\mu^2}{\prod_i m_i!} \prod_{k=1}^N \|\psi_{\mu_k}\|^2, \tag{24}$$

$$\|\psi_j\|^2 = \int_{\mathcal{D}} w(r) r^{2j} \, d\mathbf{r} = \frac{1}{n_b} \int_0^{N_b} e^{-\gamma t} (\tilde{x}^2 + t)^{\gamma Q/q} t^j \, dt, \tag{25}$$

and Z_0^* is Z^* evaluated when $Q = 0$. In the case when γ is odd, the factor $\prod_i m_i! = 1$, since due to the antisymmetry, the admitted partitions μ do not have repeated numbers.

This method can equivalently be formulated by transforming the classical problem of the one-component plasma in a quantum problem of a linear chain of interacting fermions, as explained in Refs. [27, 36]. The starting point for this method is to write the Vandermonde determinant as a Gaussian integral over Grassmann variables. The final result is again (23).

For the present work, we did some calculations up to $N = 11$ particles. The coefficients c_μ needed for the numerical calculations where kindly provided by L. Šamaj for $\gamma = 2$ up to $N = 10$ and for $\gamma = 3$ up to $N = 9$. For $\gamma = 2$ and $N = 11$, and $\gamma = 3$ and $N = 10$ and $N = 11$, we obtained the coefficients using the algorithm recently proposed by Bernevig and Regnault [37], and their Jack polynomial generator online code [38]. We now turn to the results obtained from the previous analysis, starting with the effective potential experienced by the test charge Q at large distances from the disk.

3 Long Distance Behavior

3.1 General Results at Arbitrary Couplings

As mentioned earlier, the effective interaction potential, also known as potential of mean force, $V_{\text{eff}}(x)$, has the property that $-\nabla V_{\text{eff}}$ is the mean force experienced by Q. It is interesting to introduce another quantity, $V(x)$, the electric potential created by the average charge density distribution $q(n(r) - n_b)$ at the position of the charge Q

$$V(x) = \int_{\mathcal{D}} q(n(r) - n_b) v_Q(x, r) \, d\mathbf{r}. \tag{26}$$

Because of the fluctuations and the fact that the presence of Q at position x modifies the density on the disk, in general $V_{\text{eff}}(x) \neq Q V(x)$, only for a small infinitesimal charge Q the equality holds. For arbitrary Q, a simple relation can be found between the two, by noticing that the total potential energy of the system (5) depends linearly on Q, then

$$\frac{\partial e^{-\beta H}}{\partial Q} = -\beta \int_{\mathcal{D}} q(\widehat{n}(\mathbf{r}; \mathbf{r}_1, \ldots, \mathbf{r}_N) - n_b) v_Q(x, r) \, d\mathbf{r} \, e^{-\beta H} \tag{27}$$

where $\widehat{n}(r; \mathbf{r}_1, \ldots, \mathbf{r}_N) = \sum_{i=1}^{N} \delta(\mathbf{r} - \mathbf{r}_i)$ is the microscopic density. Averaging this relation over all the configurations of the ions on the disk, we find

$$\frac{\partial V_{\text{eff}}(x)}{\partial Q} = V(x). \tag{28}$$

At large distances from the disk, expanding $v_Q(x, r)$ for $r \ll x$, one can obtain the multipolar expansion of the electric potential V

$$V(x) = -q(N - N_b) \ln \widetilde{x} - q \frac{\mathbb{Q}_2}{2x^2} + O(1/\widetilde{x}^4) \tag{29}$$

where the relevant quadrupole moment $\mathbb{Q}_2$ results from the second moment of the excess density $[n^0(r) - n_b]$

$$\mathbb{Q}_2 = \int_{\mathcal{D}} r^2 [n^0(r) - n_b] \, d\mathbf{r} \tag{30}$$

where $n^0(r)$ is the density when $x \to \infty$ (or equivalently $Q = 0$). Since we are computing the potential on the x-axis, no dipolar contribution remains, while the logarithmic monopole contribution stems from the global charge of the disk, $q(N - N_b)$. Since up to terms of higher power than $1/x^2$, (29) shows that $V(x)$ does not depend on Q, integrating (28) one finds that (29) also gives the large x expansion of V_{eff} (multiplied by Q).

We also mention here a sum rule that turns out interesting for the following discussion. The quadrupolar moment $\mathbb{Q}_2$ can be shown to be related to the mobile particle density at contact through [32, 39]

$$\Gamma \frac{n_b}{2R^2} \mathbb{Q}_2 = n_b \left(1 - \frac{\Gamma}{4}\right) - n^0(R) \tag{31}$$

for a neutral disk.

For the next order of the expansion, in $1/x^4$, the situation is more involved. The expansion of $V(x)$ cannot be obtained only from the next multipole $\mathbb{Q}_4 = \int_{\mathcal{D}} r^4(n^0(r) - n_b) \, d\mathbf{r}$, since the density $n(r)$ itself depends also on x and one needs to take into account the next-to-leading order of the large-x expansion of $n(r)$ to compute properly the expansion of $V(x)$ up to order $1/x^4$. This next-to-leading order is of order $1/x^2$ and it is proportional to Q as it can be checked by expanding $e^{-\beta H}$ for large x. It has the form

$$n(r) = n^0(r) + \frac{\beta Q q d_2(r)}{x^2} + O(1/\widetilde{x}^4) \tag{32}$$

where $d_2(r)$ is a function only of r and βq^2. Using this expansion one can obtain from (26) the expansion of $V(x)$ up to the order $1/x^4$

$$V(x) = -q(N - N_b) \ln \widetilde{x} - q \frac{\mathbb{Q}_2}{2x^2} + q \left(\frac{\mathbb{Q}_4}{4} - \frac{\beta q Q}{2} \int_{\mathcal{D}} r^2 d_2(r) \, d\mathbf{r}\right) \frac{1}{x^4} + O(1/x^6). \tag{33}$$

Then integrating with respect to Q one finds

$$V_{\text{eff}}(x) = -q Q(N - N_b) \ln \widetilde{x} - q Q \frac{\mathbb{Q}_2}{2x^2} + q Q \left(\frac{\mathbb{Q}_4}{4} - \frac{\beta q Q}{4} \int_{\mathcal{D}} r^2 d_2(r) \, d\mathbf{r}\right) \frac{1}{x^4}$$
$$+ O(1/x^6). \tag{34}$$

The term involving the second moment of d_2 differs by a factor $Q/2$ between $V(x)$ and $V_{\text{eff}}(x)$. In the following section we illustrate these considerations on the explicit results obtained when $\Gamma = \beta q^2 = 2$.

3.2 Results at $\Gamma = 2$

Unless otherwise specified, the results reported correspond to $\Gamma = 2$. For Q arbitrary, the long distance behavior of the effective interaction (15), for N and N_b fixed, $\widetilde{x}^2 \gg N$ and $\widetilde{x}^2 \gg N_b$ is

$$V_{\text{eff}}(x) = -Qq(N - N_b) \ln \widetilde{x} + \frac{Qq}{2} \frac{1}{\widetilde{x}^2} \left[\frac{N_b^2}{2} - \sum_{j=1}^{N} \frac{\gamma(j+1, N_b)}{\gamma(j, N_b)} \right]$$

$$- \frac{Q}{4\widetilde{x}^4} \sum_{j=1}^{N} \left[(Q - q) \frac{\gamma(j+2, N_b)}{\gamma(j, N_b)} - Q \frac{\gamma(j+1, N_b)^2}{\gamma(j, N_b)^2} \right] + O(1/\widetilde{x}^6), \quad (35)$$

the structure of which deserves some comments. Up to order $1/x^2$, such a series has the form of a multipolar expansion, in agreement with the discussion from the previous section. Indeed, the coefficient of $1/\widetilde{x}^2$ is precisely $-qQ\mathbb{Q}_2/2$ as it can be checked by computing the second moment of the excess density from the explicit expression (17) when $Q = 0$. Equation (35) can be compared to the large-x expansion of the electric potential

$$V(x) = -q(N - N_b) \ln \widetilde{x} + \frac{q}{2} \frac{1}{\widetilde{x}^2} \left[\frac{N_b^2}{2} - \sum_{j=1}^{N} \frac{\gamma(j+1, N_b)}{\gamma(j, N_b)} \right]$$

$$- \frac{1}{4\widetilde{x}^4} \sum_{j=1}^{N} \left[(2Q - q) \frac{\gamma(j+2, N_b)}{\gamma(j, N_b)} - \frac{\gamma(j+1, N_b)^2}{\gamma(j, N_b)^2} \right] + O(1/\widetilde{x}^6), \quad (36)$$

where one can explicitly check that $\partial_Q V_{\text{eff}} = V$.

Let us discuss further the expansion of V_{eff} up to order $1/x^2$. Using the properties of the incomplete gamma function, that allow us to write the coefficient of the $1/\widetilde{x}^2$ term appearing in (35) as

$$\frac{N_b^2}{2} - \sum_{j=1}^{N} \frac{\gamma(j+1, N_b)}{\gamma(j, N_b)} = \frac{N_b^2 - N^2}{2} - \frac{N}{2} + \sum_{j=1}^{N} \frac{e^{-N_b} N_b^j}{\gamma(j, N_b)}$$

$$= \frac{N_b^2 - N^2}{2} - \frac{N}{2} + \frac{N_b n^0(R)}{n_b}, \quad (37)$$

where $n^0(R)$ is the density of particles at the edge of the disk in the absence of the charge Q, i.e. (17) with $Q = 0$ at $\widetilde{r} = \widetilde{R} = \sqrt{N_b}$. Thus,

$$V_{\text{eff}}(x) = -Qq(N - N_b) \ln \widetilde{x} + \frac{Qq}{2} \frac{1}{\widetilde{x}^2} \left[\frac{N_b^2 - N^2}{2} - \frac{N}{2} + \frac{N_b n^{(0)}(R)}{n_b} \right] + O(1/\widetilde{x}^4). \quad (38)$$

For a neutral disk, $N = N_b$, and

$$V_{\text{eff}}(x) = \frac{Qq N_b}{2} \frac{1}{\widetilde{x}^2} \left[\frac{n^{(0)}(R)}{n_b} - \frac{1}{2} \right] + O(1/\widetilde{x}^4). \quad (39)$$

This result is an explicit check, at $\Gamma = 2$, of the multipolar expansion (29) combined with the sum rule (31). One notice that the V_{eff} is repulsive for $Qq > 0$. This can be understood as follows. When $\widetilde{x} \to \infty$, the charge density profile $n(r)$ inside the disk is the same one as for a disk alone (without the approaching charge Q), found in Refs. [24, 40]. The density $n(r)$ is equal to the background density n_b in the bulk of the disk (local neutrality in the

Fig. 2 Reduced charge density profile in the disk, for different neutral situations ($N = N_b$), and $x \to \infty$. The *arrow* on the right hand side indicates the limiting value $\ln 2 \simeq 0.693$ that is reached in the large N limit. The total charge density profile is $q[n(r) - n_b]$. For large N, it thus vanishes except in a small region of linear size $1/\sqrt{N_b}$ in the vicinity of the boundary $r = R$
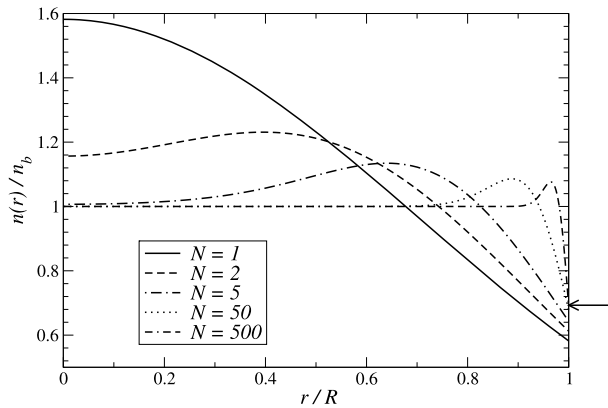
bulk). Close to the boundary, it raises above the background density, then falls below it [40], see Fig. 2. Therefore, there are two concentric layers of charges close to the edge: the inner layer bears a net charge which is of the same sign as q [i.e. $n(r) > n_b$], while the outer one is opposite, by electroneutrality. This ensures that $\mathbb{Q}_2$ is generically negative, so that the quadrupolar term yields an effective interaction (disk-test charge) that is of the same sign as Qq, i.e. repulsive for $Qq > 0$.

When $N \to \infty$, more explicit results can be obtained. In this limit, the density at the edge of the disk takes a simple form [40], $n^{(0)}(R) = n_b \ln 2$, so that

$$
\begin{aligned}
V_{\text{eff}}(x) &= \frac{QqN_b}{2} \frac{1}{\widetilde{x}^2}\left(\ln 2 - \frac{1}{2}\right) + O(1/\widetilde{x}^4) \\
&= \frac{QqR^2}{2} \frac{1}{x^2}\left(\ln 2 - \frac{1}{2}\right) + O(1/x^4),
\end{aligned} \tag{40}
$$

with $\ln 2 - \frac{1}{2} \simeq 0.19 > 0$, which is consistent with the generic discussion above on the negative sign of $\mathbb{Q}_2$. Again, the effective potential is attractive at large distances for $Qq < 0$, repulsive for $Qq > 0$, for a neutral disk.

The quadrupolar route allows us to obtain results for strongly coupled systems (large Γ), making use of the sum rule (31). We note in passing that this general result is compatible with the value $\mathbb{Q}_2 = -qR^2(\log 2 - 1/2)$ that holds at $\Gamma = 2$ when the number of mobile charges on the disk becomes large, see (40) and (29). When Γ itself turns large, the system crystallizes, but the sum rule (31) remains valid, provided $n(R)$ is replaced by the average of the contact density over the perimeter of the disk [32, 39]. It is physically reasonable to suppose that the average of $n(R)/n_b$ remains bounded in this limit. Actually, for the three-dimensional analogue of this model, with $1/r$ interaction, this is the case [41]. Then (31) becomes $\mathbb{Q}_2 \sim -R^2/2$. We consequently have

$$
V_{\text{eff}}(x) \underset{\Gamma \to \infty}{\sim} \frac{QqR^2}{4} \frac{1}{x^2} + O(1/x^4), \tag{41}
$$

which is again repulsive for $Qq > 0$, attractive otherwise. It can be mentioned here that the scaling result $\mathbb{Q}_2 \propto -R^2$ is readily recovered by the two concentric layers simplified viewpoint. For large N, there exists a outermost corona void of charges: particles are depleted there, as they are in the plum pudding model, see e.g. [21, 22, 41], the width of which is given by the typical distance between particles $\delta \propto R/\sqrt{N}$ (at $\Gamma = 2$, δ is already the typical distance between the density maximum and the disk radius that can be seen in Fig. 2

for large N). The charge in this corona is given by $-qn_bR\delta$, which contributes a quantity $-Rn_b\,\delta\,R^2$ to the quadrupole moment. This charge is compensated by an oppositely charged ring, located at $R-\delta$, which contributes a quantity $R\,\delta\,n_b(R-\delta)^2$ to $\mathbb{Q}_2$. Summing both contributions, assuming that the particles and background with $r < R-\delta$ do not contribute to $\mathbb{Q}_2$, and remembering that $\delta \ll R$, we arrive at $\mathbb{Q}_2 \propto -n_bR^2\delta^2 \simeq -R^2$. A very similar argument holds at $\Gamma = 2$, since the two corona approach is also valid.

4 Short Scale Features

We now turn to the study of the phenomenology at shorter distances, which is different depending on whether the particle approaching the disk has a charge of the same sign of the mobile particles on the disk ($Q/q > 0$), or a charge of opposite sign. In addition, the cases of globally neutral or charged disks should be treated separately, and the different cases are ruled by different sorts of polarization effects.

4.1 Case $Q/q > 0$

4.1.1 Neutral Disk

We consider a globally neutral disk $N = N_b$. We study in this section if it is possible to overcharge this object, by approaching a particle that has a charge Q with the same sign of the mobile counterions on the disk. At large distances, we know from (38) that the interaction is repulsive. We anticipate that this behavior changes when the charge Q is close enough to the disk, since the intruder Q should then create a correlation hole, pushing mobile charges closer to the boundary $r = R$, and thereby gaining Coulombic energy from hole opened. This is the mechanism behind charge inversion in colloidal systems, that has been reviewed for situations of strong coupling in Ref. [3].

The short-distance behavior of the effective potential (15) is, when $Q/q > 0$,

$$\beta V_{\text{eff}}(x) = \frac{Q}{q}\left[N_b \ln N_b - N_b + \widetilde{x}^2\left(1 + \ln\frac{N_b}{\widetilde{x}^2}\right)\right] - \sum_{j=1}^{N}\ln\frac{\gamma(j+\frac{Q}{q},N_b)}{\gamma(j,N_b)}$$
$$- \frac{Q}{q}\widetilde{x}^2\sum_{j=1}^{N}\frac{\gamma(j+\frac{Q}{q}-1,N_b)}{\gamma(j+\frac{Q}{q},N_b)} + O\left(\widetilde{x}^4,\widetilde{x}^{2(1+Q/q)}\right), \tag{42}$$

which is clearly an increasing function of x when $\widetilde{x} \ll 1$. Therefore, at close distance from the disk, the interaction turns out to be attractive. This can be observed in Fig. 3, where the effective potential indeed increases at short distances, reaches a maximum and then decreases upon increasing the distance between the test particle and the disk. Note that at $x = 0$, the effective potential takes a finite value

$$\beta V_{\text{eff}}(0) = \frac{Q}{q}(N_b \ln N_b - N_b) - \sum_{j=1}^{N}\ln\frac{\gamma(j+\frac{Q}{q},N_b)}{\gamma(j,N_b)}, \tag{43}$$

although it is not shown in all figures.

Let x^* be the distance at which the interaction potential reaches its maximum, and $\widetilde{x}^* = \sqrt{\pi n_b}x^*$. x^* is the minimum distance that one has to approach the charged particle in order to overcome the natural repulsion of the disk. The corresponding (free) energy cost to overcharge the disk is given by $V^\dagger = V_{\text{eff}}(x^*)$, and $V^* = V^\dagger - V_{\text{eff}}(0)$ is the binding
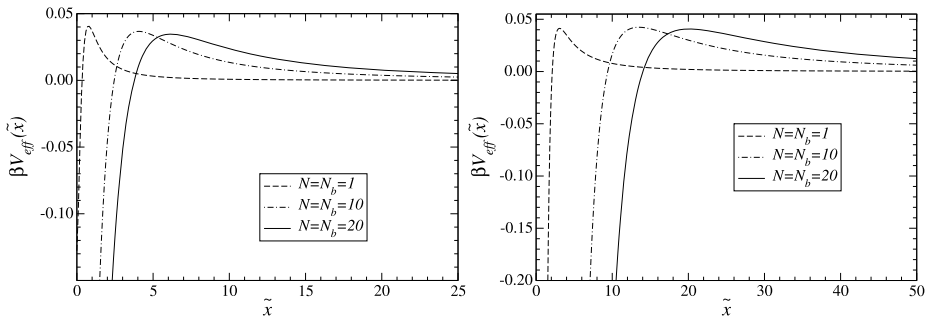
Fig. 3 The effective interaction between the disk and an approaching ion with charge $Q = q$ (*left graph*) or $Q = 10q$ (*right graph*). The disk is globally neutral with $N_b = N$ ions of charge q. The distance x is expressed in reduced units ($\tilde{x}$), in which the disk radius reads $\sqrt{N_b}$, and therefore takes different values for the three curves shown
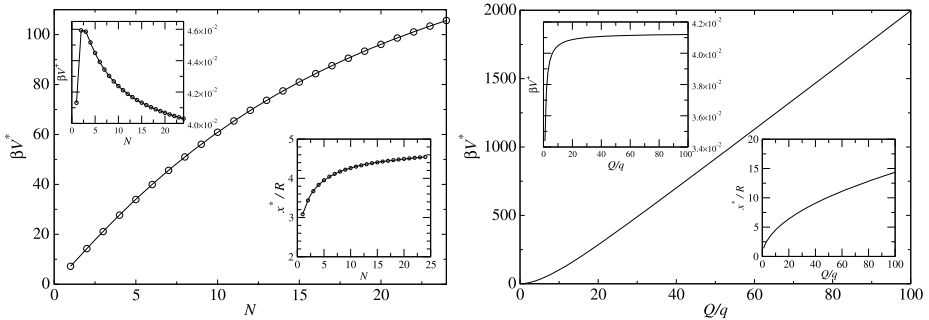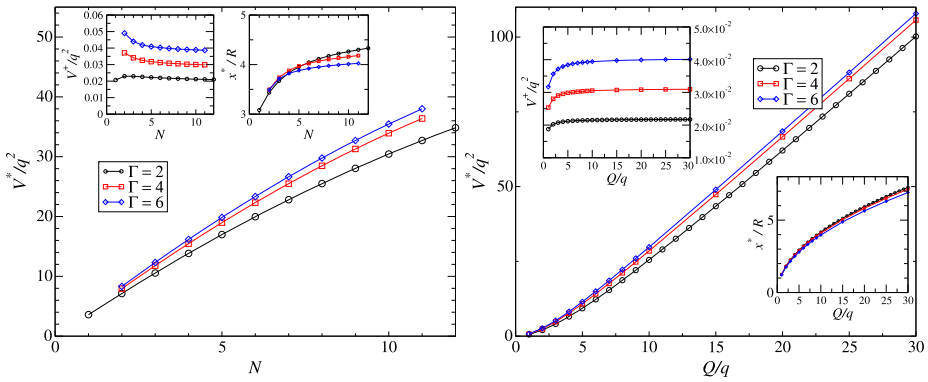

Fig. 4 *Left*: The binding energy V^*, the energy cost $V^\dagger$ and the distance x^* to overcharge the globally neutral disk with an additional particle of charge $Q = 10q$, as a function of the number of particles $N = N_b$ on the disk. *Right*: Same quantities as a function of intruder charge Q, for $N = N_b = 22$

energy, i.e. the necessary energy to unbind the charged particle from the disk, once it has been overcharged. More generally, V^* can be defined as the energy to overcome to peel off an ion from the disk. In all the present discussion, the energy costs alluded to correspond to the work an external operator holding the intruder should perform, and this equals the corresponding free energy variation of the system as a whole.

Figure 4 shows how x^*/R, $V^\dagger$ and V^* depend on N for fixed Q/q, and on Q/q at fixed N, respectively. First of all, it appears that the binding energy V^* is several orders of magnitude larger than the energy cost $V^\dagger$. This means that $V^* \simeq |V_{\mathrm{eff}}(0)|$. Second, the threshold distance x^* scales like R, when N becomes large enough, a fact that is masked in Fig. 3 by the choice of units made (tilde variables, for which $\tilde{R} = \sqrt{N_b}$). More precisely, from the numerical data of Fig. 4, we explored how x^*/R depends on the charge Q. We found, numerically, the approximate relation

$$\frac{x^*}{R} = a\sqrt{\frac{Q}{q}} + O(1/\sqrt{N}) \qquad (44)$$

with $a = 1.5 + O(1/\sqrt{N})$. The fact that a is of order one means that the effect of effective attractions holds up to rather large distances, on the order of the disk radius. Another feature visible on Fig. 4 is that the energy cost increases with Q/q, but quickly saturates to a finite

Fig. 5 *Left*: The binding energy V^*, the energy cost $V^\dagger$ and the distance x^* to overcharge the globally neutral disk with an additional particle of charge $Q = 10q$ as a function of the number of particles $N = N_b$ on the disk, for different values of the Coulombic coupling $\Gamma = \beta q^2$. *Right*: Same as a function of Q, for a globally neutral disk with $N = N_b = 8$

value $V_{\text{eff}}^{\text{sat}}$. On the other hand the binding energy increases as the charge Q increases, as expected, but it also increases with the number of mobile ions on the disk N. For $N \to \infty$, using Stirling formula for the incomplete gamma functions in (43), one can obtain the analytical behavior of $V_{\text{eff}}(0)$, and therefore the one of the binding energy, remembering that $V^* \simeq |V_{\text{eff}}(0)|$. We find

$$\beta V_{\text{eff}}(0) = -\frac{1}{2}\left(\frac{Q}{q}\right)^2 \ln N + O(1). \tag{45}$$

Figure 5 shows how the previous quantities behave under different couplings ($\Gamma = \beta q^2 = 2, 4, 6$). The qualitative features appear to be robust: The behavior is similar to the one when $\Gamma = 2$, with changes in the numerical values of x^*, $V^\dagger$ and V^*. As Γ increases, $V^\dagger$ and V^* increase, and x^* decreases slightly: the test ion has to come closer to the disk, and requires more energy to overcome the long distance repulsion. Once it overcharges the disk it is more energetically bounded to it.

4.1.2 Charged Disk

If $N < N_b$, the disk has a charge $q(N - N_b)$ of opposite sign to that of the approaching ion Q. In this case the effective potential is attractive at all distances. Let us consider the more interesting case where the disk is already overcharged, with a net charge of the same sign as Q, i.e. $N > N_b$. The question is to study the effective potential profile, and the distance range where it corresponds to an effective attraction.

At large distances, the effective interaction between the ion and the disk is repulsive, and diverges as $-Qq(N - N_b) \ln \widetilde{x}$. However, from (42), we find that, at short distances, the effective potential becomes attractive. Therefore, as in the previous situation, there exists a distance x^* below which the test charge will be attracted, which results in a further charge inversion of the disk. Figure 6 shows the effective potential in this situation for different charges Q and charges of the disk $q(N - N_b)$. Here, one can also define a binding energy $V^* = V_{\text{eff}}(x^*) - V_{\text{eff}}(0)$, necessary to pull out the ion from the disk once it has been "adsorbed". Figure 7 shows how x^* and V^* depend on the charge Q of the ion and on the charge of the disk, respectively. It is also useful to emphasize that when the disk complex

Fig. 6 The effective potential between the charged disk and the approaching ion in cases where $Q/q > 0$ and where the large distance behaviour is repulsive (i.e. $N > N_b$). The *main inset* is for $N_b = 15$, $N = 16$, $Q/q = 5$ while the *smaller inset* is for $N_b = 10$, $N = 16$, $Q/q = 1$
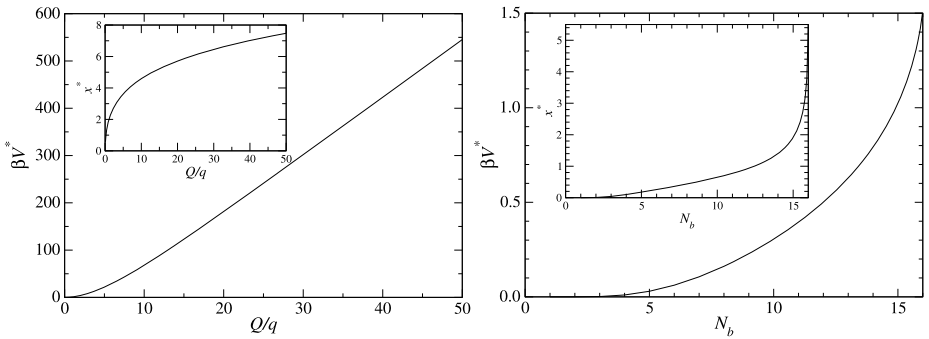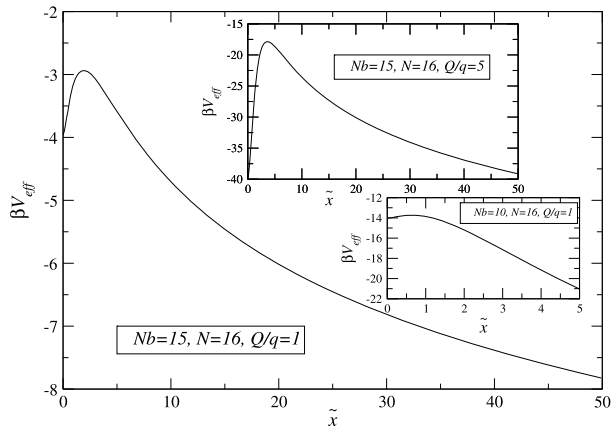

Fig. 7 *Left*: The binding energy V^* and the distance x^* to overcharge the charged disk with $N_b = 15$ and $N = 16$ particles (global charge q) with an additional charged particle with charge Q as a function of Q/q. *Right*: Same, as a function of N_b, for $N = 16$ and $Q = q$

is not neutral, one cannot define the energy barrier $V^\dagger$. Indeed, this quantity was defined in the neutral case as the barrier to overcome to approach the test charge from $x = \infty$, down to the distance where attraction sets in. When $N \neq N_b$, the large distance effective potential diverges as $(N - N_b) \log x$, which precludes the definition of $V^\dagger = V_{\text{eff}}(x^*) - V_{\text{eff}}(\infty)$. This feature is absent in three dimensions, where charges interact though a $1/r$ potential (hence the possible definition of $V^\dagger$ also for non-neutral complexes). As a consequence, the study of overcharging is somewhat less rich in the present case than for three dimensional systems and overcharging is, with a log potential, necessarily a phenomenon of small amplitude (if not infinitesimal): another way to rephrase previous remarks is that $V^\dagger$ diverges as soon as $N \neq N_b$.

To understand the mechanism behind the attraction at short distances, it is instructive to study the density distribution of particles in $\mathcal{D}$, as Q approaches the disk. Figure 8 shows the density profile for different distances x. It can be seen that the correlation hole alluded to earlier is increasingly marked, when x becomes smaller: the mobile charges q of the disk feel the repulsion due to the charge Q, and move towards the edge of the disk. This results in a local negative charge density in the center of the disk, which is finally responsible for the attractive interaction between the disk and the intruder charge Q.

Fig. 8 The density profile of mobile particles in the disk, with $N = 16$, $N_b = 15$, charge of the disk equal to q and the approaching ion has charge $Q = 5q$. Notice that as the ion approaches the disk, the charge density in the center of the disk becomes negative. This results in the effective attraction at short-distances x of the disk and the ion
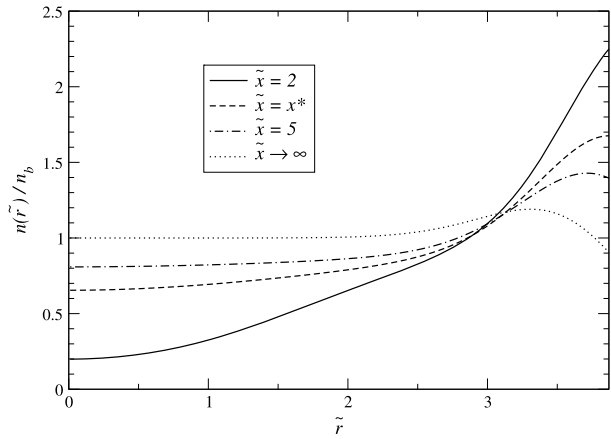
Fig. 9 The effective potential between the globally neutral disk and the approaching ion, in the case where the charge of the test ion and those of the mobile particles on the disk have opposite signs: $Q/q < 0$. Here, the disk bears $N = 10$ particles with charge q
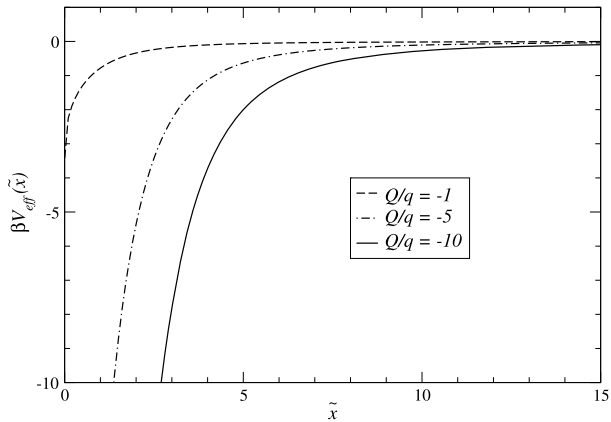

4.2 Case $Q/q < 0$

We now turn to the case where the test particle and mobile ions on the disk have charges of opposite signs.

4.2.1 Neutral Disk

For a globally neutral disk ($N = N_b$), we know from (39) and the analysis of Sect. 3 that the effective potential is attractive at large-distances. This behavior remains at short-distances, as illustrated in Fig. 9. Therefore, the neutral disk has a natural tendency to overcharge.

4.2.2 Charged Disk

If $N > N_b$, the disk has a charge $q(N - N_b)$ of opposite sign as the approaching ion Q. In this case the effective potential is always attractive, a situation that is not of particular interest. We concentrate instead on the case where the disk has a net charge of the same sign as Q, i.e. $N_b > N$. Due to this excess charge, the effective potential with a charge Q of the same sign as the disk is expected to be repulsive at large distances, see (38). However, as
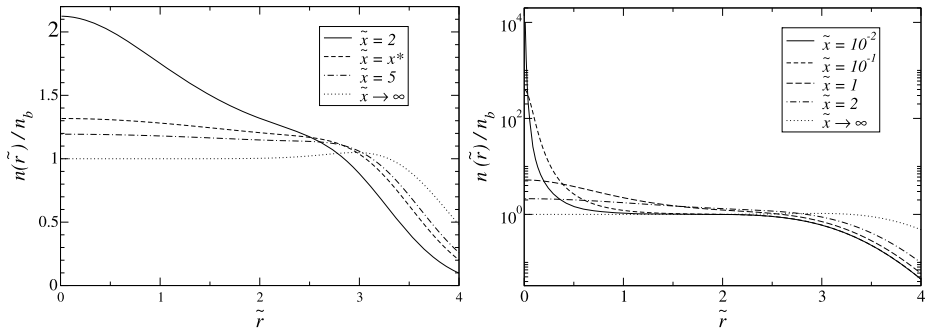
Fig. 10 Density profile of counterions in the disk, in the case $Q = -5q$, with $N = 15$ and $N_b = 16$. The net charge of the disk is then equal to $-q$

we shall see below, there is here also a change in the behavior of the effective interaction at short distances, where the force between the disk and the particle becomes attractive.

The situation seems at first sight similar to the case studied in Sect. 4.1. There are some notable differences though. If $Q/q \leq -1$, the effective potential diverges when $\widetilde{x} \to 0$. Indeed, for $Q/q \leq -1$, (42) is no longer valid. The dominant contribution is given by the term $j = 1$ in the sum (15). Explicitly, it yields, for $Q/q < -1$,

$$V_{\text{eff}}(x) \sim -q(Q + q) \ln \widetilde{x}, \quad x \to 0 \tag{46}$$

and

$$V_{\text{eff}}(x) \sim -\frac{q^2}{2} \ln\left(\ln \frac{1}{\widetilde{x}}\right), \quad x \to 0, \tag{47}$$

if $Q = -q$. In both cases, the small x behaviour is attractive. We note that the divergence of $V_{\text{eff}}(x)$ for $x \to 0$ stems from the fact that the Boltzmann weight $\exp(\beta Qq \log r) = 1/r^{-\Gamma Q/q}$ is non-integrable at $r = 0$ whenever $Q/q < -2/\Gamma$. As announced earlier, the effective potential is repulsive at large distances and attractive at short distances. We can thus again define the distance x^* at which the potential becomes attractive if we approach the ion below x^*. However, in the present case, the binding energy V^* is infinite because $\lim_{x \to 0} V_{\text{eff}}(x) = -\infty$. Likewise, we cannot define the energy barrier $V^\dagger$ since either attraction applies at all distances (neutral complex on the disk), or the effective potential diverges at infinity (charged case).

The mechanism behind the attraction between these like-charged objects at short distance is now due to an accumulation of mobile charges near the center of the disk. This can be seen in Fig. 10, which shows the density profile of the mobile charges q, i.e. the counterions. As the charge Q approaches, it strongly attracts the counterions to the disk center, and this results in an effective attraction, the precise form of which is non-trivial. As seen on Fig. 10, for small $\widetilde{x}$, there is a large density of counterions close to the center of the disk, but which is concentrated over a disk of radius of order 1 in $\widetilde{r}$ units. The precise analytical behavior of the charge density can be extracted from (17), for $\widetilde{x} \ll 1$, taking into account that for $Q/q < -1$ the first term of the sum is the dominant one

$$n(r) \sim -n_b e^{-\widetilde{r}^2} \left(\frac{Q}{q} + 1\right)\left(1 + \frac{\widetilde{r}^2}{\widetilde{x}^2}\right)\frac{1}{\widetilde{x}^2}. \tag{48}$$

The total integrated charge of this counterion cloud close to the center plus the background turns out to be equal to $-Q$, as one might expect. However, the behaviour of the effective

potential encoded in (46) and (47) exhibits a different attraction than the bare Coulombic form $-Q^2 \log \widetilde{x}$, that would be obtained assuming the attracted counterions are located as a point charge at $r = 0$. Since they are spread over distances larger than $\widetilde{x}$, the behavior of the potential, although logarithmic, turns out to have a different prefactor, see (46).

The case when $-1 < Q/q < 0$ is somewhat different. The effective interaction potential is no longer logarithmic and has a finite value at $x = 0$. For $x \to 0$,

$$\beta V_{\text{eff}}(x) = \beta V_{\text{eff}}(0) + \frac{\widetilde{x}^{2(1+Q/q)}}{(\frac{Q}{q}+1)\gamma(1+Q/q, N_b)} + O(\widetilde{x}^2) \qquad (49)$$

with $V_{\text{eff}}(0)$ given by (43). Notice that since $0 < 1 + Q/q < 1$, the potential is again attractive at short distances. Also the power law $\widetilde{x}^{2(1+Q/q)}$ is different from the one of the case $Q/q > 0$ where it was $\widetilde{x}^2$. In this case, $-1 < Q/q < 0$, it is again possible to define the binding energy, that diverges when the limit $Q/q \to -1^+$ is approached. One can indeed show that $\beta V_{\text{eff}}(0) \sim \ln(1 + Q/q)$.

5 Conclusion and Discussion

We have introduced a classical system that exhibits some of the phenomenology at work in more complex colloidal suspensions. An ensemble of N point particles with charge q are free to move within a disk of radius R, that bears a uniform background charge of surface density $-q N_b/(\pi R^2)$. The corresponding complex (mobile charges and background) forms a one component plasma, with a global charge $(N - N_b)q$. A test point charge Q is then approached to the complex, perpendicularly to the disk plane, along its axis of symmetry (x-axis, see Fig. 1). All charges were assumed to interact through a log potential, a choice that is convenient for the derivation of analytical results and for the discussion of the physical mechanisms, but that we emphasized as somewhat irrealistic for a real Coulombic problem in three dimensions. We have studied in detail the x-dependent effective potential V_{eff} experienced by the intruder Q, defined as the free energy of the complete charge distribution for a given distance x between the test charge and the complex.

At short distances x, V_{eff} is always attractive, with different underlying mechanisms depending on the sign of Q/q. If the intruder and the mobile charges are like-charged, the intruder creates its own correlation hole as it approaches the disk. The resulting short-range attraction resulting from this polarization is analogous to its three dimensional counterpart explaining charge inversion (overcharging, see Ref. [3]). If on the other hand $Q/q < 0$, the test particle attracts an excess of mobile charges in the vicinity of the disk center, which overcomes the background—test charge repulsion. In this case, we found a diverging attraction for $Q/q \leq -1$, which precludes the definition of a binding energy (cost to drag the test charge away from the disk, starting from $x = 0$, the point of contact).

The long distance behaviour is also of interest. If the complex has a net charge, the leading contribution to V_{eff} reads $-Qq(N - N_b) \ln \widetilde{x}$, which leads to the expected like-charge repulsion at large x. The neutral case $N = N_b$ is more subtle, and it has been shown that a key quantity to rationalize V_{eff} is the quadrupolar moment $\mathbb{Q}_2$ of the total charge distribution on the disk. At large x, polarization effects disappear, and the mobile charges adopt a profile that compensates for the background charge in the bulk of the disk, while they are expelled from the immediate vicinity of the disk edge $r = R$, thereby creating a charge imbalance far from the disk center only. This necessarily leads to a negative value of $\mathbb{Q}_2$, and hence to a repulsive behaviour at large x, when $Q/q > 0$. Indeed, what matters for large distance interactions is the charges that are closest to the intruder, and they happen to be the mobile
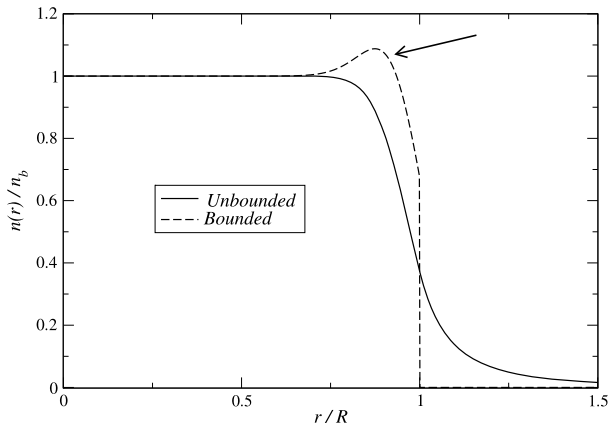
Fig. 11 Density profile of counterions in the disk, for the "unbounded" and "bounded" models (counter-ions are either allowed to explore the region $r > R$, or not). Here $N = N_b = 40$ and $\Gamma = 2$. The counter-ion excess for the bounded model—shown by the *arrow*, and studied extensively in this paper—leads to a negative quadrupole moment $\mathbb{Q}_2$, see Sect. 3, while in the unbounded case, one mobile ion escapes to infinity, leaving the complex (disk + ions) with a net charge $-q$. This results in large distance effective forces on the test charge that have opposite signs

charges expelled from $r = R$ (see the region where $n > n_b$ in Fig. 2, for $N = 50$ or $N = 500$, or equivalently, see the arrow in Fig. 11). The ensuing interaction is repulsive when Q and q are of the same sign. This leads us to a final remark that illustrates the subtlety of the long distance effective potential. Consider a variant of the previous model, where the mobile charges are no longer confined in the disk $r < R$, but can explore the full disk plane (they are thus still 2D confined, but unbounded in the plane). The uniform background, as before, is a disk of radius R. We can repeat the analysis for $\Gamma = 2$, which leads to a profile $n(r)$ that departs from the one reported above in an essential way: As can be seen in Fig. 11, it is monotonously decreasing, as happens to be the case at mean-field level [42] (i.e. for $\Gamma \to 0$). For $N \geq N_b$, the decay of the density profile $n(r)$ at large distances is algebraic in $1/r^4$ [43, 44], leading to a divergent quadrupole. Furthermore, the density profile of this "unbounded" model shows a peculiarity, when $N \geq N_b$, $\int_{\mathbb{R}^2} n(r) \, d^2\mathbf{r} = N_b - 1$. Since there were originally N mobile particles, this means that $N - N_b + 1$ particles have escaped to infinity. This can be checked explicitly at $\Gamma = 2$ [43–45], but more generally, it is a manifestation of the Onsager-Manning-Oosawa condensation phenomenon [46–48]: only a fraction $(N_b - 1)/N_b$ of the mobile ions are "condensed" inside or in the vicinity of the disk. This is a consequence of the logarithmic interaction between the ions and the disk when they are outside the disk. As a consequence, and at variance with the bounded model where the charges stay in the disk, the global charge of the complex (disk + mobile ions) is $-q$, whenever $N \geq N_b$. Therefore one expect that the effective interaction of this complex with the charge Q at large x will be attractive for $Q/q > 0$. This situation is opposite to the one met with the bounded model.

References

1. Gelbart, W., Bruinsma, R., Pincus, P., Parsegian, A.: Phys. Today **53**, 38 (2000)
2. Hansen, J.-P., Löwen, H.: Annu. Rev. Phys. Chem. **51**, 209 (2000)
3. Grosberg, A.Y., Nguyen, T., Shklovskii, B.: Rev. Mod. Phys. **74**, 329 (2002)
4. Levin, Y.: Rep. Prog. Phys. **65**, 1577 (2002)
5. Levin, Y.: Physica A **353**, 43 (2005)
6. Messina, R.: J. Phys., Condens. Matter **21**, 113102 (2009)
7. Naji, A., Kanduč, M., Netz, R., Podgornik, R.: In: Andelman, D., Reiter, G. (eds.) Understanding Soft Condensed Matter via Modeling and Computation. Addison Wesley, Reading (2010)
8. Trizac, E.: Phys. Rev. E **62**, R1465 (2000)
9. Rouzina, I., Bloomfield, V.: J. Phys. Chem. **100**, 9977 (1996)
10. Shklovskii, B.I.: Phys. Rev. E **60**, 5802 (1999)
11. Moreira, A., Netz, R.: Eur. Phys. J. E **8**, 33 (2002)
12. Boroudjerdi, H., Kim, Y.-W., Naji, A., Netz, R., Schlagberger, X., Serr, A.: Phys. Rep. **416**, 129 (2005)
13. Šamaj, L., Trizac, E.: Phys. Rev. Lett. **106**, 078301 (2011)
14. Gouy, D.: J. Phys. **9**, 457 (1910)
15. Chapman, D.: Philos. Mag. **6**, 475 (1913)
16. Burak, Y., Andelman, D., Orland, H.: Phys. Rev. E **70**, 016102 (2004)
17. Chen, Y.-G., Weeks, J.: Proc. Natl. Acad. Sci. USA **103**, 7560 (2006)
18. Santangelo, C.D.: Phys. Rev. E **73**, 041512 (2006)
19. Buyukdagli, S., Manghi, M., Palmeri, J.: Phys. Rev. Lett. **105**, 158103 (2010)
20. Thomson, J.: Philos. Mag. **7**, 237 (1904)
21. Bedanov, V., Peeters, F.: Phys. Rev. B **49**, 2667 (1994)
22. Chepelianskii, A., Closa, F., Raphaël, E., Trizac, E.: Europhys. Lett. **94**, 68010 (2011)
23. Deutsch, C., Lavaud, M.: Phys. Rev. A **9**, 2598 (1974)
24. Jancovici, B.: Phys. Rev. Lett. **46**, 386 (1981)
25. Hunter, R.: Foundations of Colloid Science. Oxford University Press, London (2001)
26. Alastuey, A., Jancovici, B.: J. Phys. France **42**, 1 (1981)
27. Šamaj, L.: J. Stat. Phys. **117**, 131 (2004)
28. Zabrodin, A., Wiegmann, P.: J. Phys. A **39**, 8933 (2006)
29. Mehta, M.: Random Matrices. Academic Press, San Diego (1991)
30. Belloni, L.: J. Phys., Condens. Matter **12**, 549 (2000)
31. Šamaj, L., Percus, J.K., Kolesík, M.: Phys. Rev. E **49**, 5623 (1994)
32. Téllez, G., Forrester, P.: J. Stat. Phys. **97**, 489 (1999)
33. Di Francesco, P., Gaudin, M., Itzykson, C., Lesage, F.: Int. J. Mod. Phys. A **9**, 4257 (1994)
34. Dunne, V.: Int. J. Mod. Phys. B **7**, 4783 (1994)
35. Scharf, T., Thibon, J.-Y., Wybourne, B.: J. Phys. A **27**, 4211 (1994)
36. Šamaj, L., Percus, J.: J. Stat. Phys. **80**, 811 (1995)
37. Bernevig, B., Regnault, N.: Phys. Rev. Lett. **103**, 206801 (2009)
38. URL: http://www.nick-ux.org/~regnault/jack/
39. Choquard, P., Favre, P., Gruber, C.: J. Stat. Phys. **23**, 405 (1980)
40. Jancovici, B.: J. Stat. Phys. **28**, 43 (1982)
41. Hasse, R., Avilov, V.: Phys. Rev. A **44**, 4506 (1991)
42. Chepelianskii, A., Mohammad-Rafiee, F., Trizac, E., Raphaël, E.: J. Phys. Chem. B **113**, 3743 (2009)
43. Jancovici, B.: J. Phys. France **47**, 389 (1986)
44. Jancovici, B.: J. Stat. Phys. **110**, 879 (2003)
45. Fantoni, R., Jancovici, B., Téllez, G.: J. Stat. Phys. **112**, 27 (2003)
46. Manning, G.S.: J. Chem. Phys. **51**, 924 (1969)
47. Manning, G.S.: J. Chem. Phys. **51**, 934 (1969)
48. Oosawa, F.: Polyelectrolytes. Dekker, New York (1971)
49. Wall, F., Berkowitz, J.: J. Chem. Phys. **26**, 114 (1957)